



Contents lists available at ScienceDirect

Journal of Traditional and Complementary Medicine

journal homepage: <http://www.elsevier.com/locate/jtcme>

## Zhilong Huoxue Tongyu capsule alleviates myocardial fibrosis by improving endothelial cell dysfunction



Tao Bi <sup>a, c, 1</sup>, Yanan Zhou <sup>a, c, 1</sup>, Linshen Mao <sup>e</sup>, Pan Liang <sup>a, c, d</sup>, Jiali Liu <sup>a, c</sup>, Luyin Yang <sup>a, c</sup>, Guilin Ren <sup>a, c</sup>, Maryam Mazhar <sup>a, b, c</sup>, Hongping Shen <sup>a, c</sup>, Ping Liu <sup>e</sup>, Roman Spáčil <sup>f</sup>, Qing Guo <sup>a, c</sup>, Gang Luo <sup>e, \*\*\*</sup>, Sijin Yang <sup>a, b, c, d, \*\*</sup>, Wei Ren <sup>a, b, c, \*</sup>

<sup>a</sup> National Traditional Chinese Medicine Clinical Research Base and Drug Research Center of the Affiliated Traditional Chinese Medicine Hospital of Southwest Medical University, Luzhou, 646000, China

<sup>b</sup> The National T.C.M Service Export Base of the Affiliated T.C.M Hospital of Southwest Medical University, Luzhou, 646000, China

<sup>c</sup> Institute of Integrated Chinese and Western Medicine, Southwest Medical University, Luzhou, 646000, China

<sup>d</sup> State Key Laboratories for Quality Research in Chinese Medicines, Faculty of Chinese Medicine, Macau University of Science and Technology, Macau, 853, China

<sup>e</sup> Department of Cardiovascular Medicine, The Affiliated Traditional Chinese Medicine Hospital of Southwest Medical University, Luzhou, Sichuan, China

<sup>f</sup> The Czech Center for Traditional Chinese Medicine, Jeremenkova 1211/40, Olomouc, 77900, Czech Republic

### ARTICLE INFO

#### Article history:

Received 29 March 2023

Received in revised form

6 June 2023

Accepted 6 July 2023

Available online 12 July 2023

#### Keywords:

Endothelium

Dysfunction

Myocardial

Fibrosis

Zhilong huoxue tongyu

Capsule

Endothelial-to-mesenchymal

Transition

MHC

Class-II

### ABSTRACT

**Background and aim:** Zhilong Huoxue Tongyu (ZL) capsule is a classical traditional Chinese medicine (TCM) with satisfactory curative effects. Endothelial cell (EC) dysfunction plays an important role during myocardial fibrosis (MF). But the therapeutic effect of ZL capsule on EC dysfunction remains unknown in the development of MF. This study aims to investigate the effect of ZL capsule on EC dysfunction during MF *in vivo*.

**Experimental procedure:** The model of MF is established *in vivo* by injecting isoproterenol for 14 days, simultaneously, we examined the therapeutic effect of ZL capsule on MF *in vivo*. An integrative approach combining biomarker examination, echocardiography and myocardial fibrosis condition using Hematoxylin-eosin staining, Masson staining, and Sirius red staining were performed to assess the efficacy of ZL capsule against MF. Subsequently, comprehensive immunofluorescence staining was performed to evaluate the therapeutic effect of ZL capsule on EC dysfunction.

**Results and conclusion:** Prior to experiments, analysis of the published single-cell sequencing data was performed and it was discovered that EC dysfunction plays an important role. Further pharmacological results showed that ZL capsule could alleviate fibrosis injury and collagen fiber deposition. The mechanism investigation results showed that the endothelial-to-mesenchymal transition (EndMT) and MHC class-II (MHC-II) expression in EC were improved. In addition, ZL capsule can attenuate the inflammatory response during MF by intervening the activation of CD4<sup>+</sup>T cell mediated by EC. For the first time, we provided evidence that ZL capsule could improve MF by alleviating EC dysfunction via the regulation of EndMT and expression of MHC-II.

**Taxonomy (classification by evis):** Myocardial fibrosis, Chinese Herbal Medicine, Traditional Medicine, Endothelium, dysfunction, Endothelial-to-mesenchymal transition.

© 2023 Center for Food and Biomolecules, National Taiwan University. Production and hosting by Elsevier Taiwan LLC. This is an open access article under the CC BY-NC-ND license (<http://creativecommons.org/licenses/by-nc-nd/4.0/>).

\* Corresponding author. 182# chunhui road, Luzhou, Sichuan, 646000, China.

\*\* Corresponding author. 182# chunhui road, Luzhou, Sichuan, 646000, China.

\*\*\* Corresponding author. 182# chunhui road, Luzhou, Sichuan, 646000, China.

E-mail addresses: [bitao456321@163.com](mailto:bitao456321@163.com) (T. Bi), [18703667421@163.com](mailto:18703667421@163.com) (Y. Zhou), [maolinshen@swmu.edu.cn](mailto:maolinshen@swmu.edu.cn) (L. Mao), [xnydzyylp@swmu.edu.cn](mailto:xnydzyylp@swmu.edu.cn) (P. Liang), [liujiali@swmu.edu.cn](mailto:liujiali@swmu.edu.cn) (J. Liu), [yangly2021@swmu.edu.cn](mailto:yangly2021@swmu.edu.cn) (L. Yang), [renguilin18@126.com](mailto:renguilin18@126.com) (G. Ren), [hanmaya@126.com](mailto:hanmaya@126.com) (M. Mazhar), [15082068899@163.com](mailto:15082068899@163.com) (H. Shen), [helloliuping@swmu.edu.cn](mailto:helloliuping@swmu.edu.cn) (P. Liu), [roman@czcn.eu](mailto:roman@czcn.eu) (R. Spáčil), [8864266@qq.com](mailto:8864266@qq.com) (Q. Guo), [1982luogang@163.com](mailto:1982luogang@163.com) (G. Luo), [ysjimm@sina.com](mailto:ysjimm@sina.com) (S. Yang), [renwei1991@swmu.edu.cn](mailto:renwei1991@swmu.edu.cn) (W. Ren).

Peer review under responsibility of The Center for Food and Biomolecules, National Taiwan University.

<sup>1</sup> These authors contributed equally to this work.

**Abbreviations:**

CVDs	cardiovascular diseases
ZL:	Zhilong Huoxue Tongyu
OCT gel	optimal cutting temperature gel
TCM	traditional Chinese medicine
MF	Myocardial fibrosis
EC	Endothelial cell
ISO	Isoproterenol
EndMT	endothelial-to-mesenchymal transition
MHC-II	MHC class-II
EF%	Ejection fraction
FS%	fractional shorting
LVEDd	left ventricular end-diastolic diameter
LVESd	left ventricular end-systolic diameter
H&E	Hematoxylin-Eosin
Masson	Masson's trichrome

**1. Introduction**

Cardiovascular disease (CVD) has become a threat to human health worldwide due to its increasing prevalence, poor prognosis and high mortality.<sup>1</sup> Epidemiologic data suggest that the number of CVDs patients worldwide has increased every year, from 271 million in 1990 to 523 million in 2019.<sup>2</sup> Growing evidence has revealed that the myocardial fibrosis (MF) is a common pathological feature of a variety of end-stage CVDs, MF is the foundation of the occurrence and development of heart failure.<sup>3</sup> Myocardial fibrosis is characterized by accumulation of activated fibroblasts and excessive deposition of fibrotic extracellular matrix proteins, among which chronic inflammation and endothelial cell (EC) dysfunction are important predisposing factors for the development of myocardial fibrosis.<sup>4</sup> EC is important in maintaining structural and functional roles of blood vessels,<sup>5</sup> which is important to maintain the normal physiological function of the heart. EC are highly sensitive to vascular pathological changes. For example, when EC is exposed to different milieus include cardiac overload and chronic hypertension, the normal function of EC changes, resulting in EC dysfunction.<sup>6</sup> In fact, EC dysfunction contributes to MF progression by promoting inflammation, activating cardiac fibroblasts and promoting the excessive deposition of collagen-I.<sup>7</sup>

Endothelial-mesenchymal transition (EndMT) is the primary mechanism resulting in EC dysfunction, which throughout the whole process of CVDs.<sup>8</sup> In this process, EC obtains characteristics of mesenchymal cells and loses the characteristics of EC.<sup>9</sup> The expression of various intercellular junction molecules in the vascular endothelium including VE-cadherin and ZO-1 decreases during EndMT,<sup>10</sup> resulting in increased vascular permeability, increased leakage, and weakened blood perfusion capacity, thereby aggravating tissue hypoxia, causing massive cell death, and destroying normal organ tissue structure.<sup>11</sup> All of these pathogenic alterations accelerate the onset of MF.<sup>12</sup> Therefore, the discovery and verification of potential therapeutic drugs targeting EndMT is crucial in the treatment of MF.

Another element contributing to EC dysfunction is the interaction between CD4<sup>+</sup>T cell activation and MHC-II expression in EC.<sup>13,14</sup> The CD4<sup>+</sup>T cell can influence fibrosis progression and scarring in multiple ways,<sup>15</sup> among which, the acceleration of inflammation by CD4<sup>+</sup>T cell has attracted increasing attention.<sup>16</sup> In

particular, persistent inflammation mediated by CD4<sup>+</sup>T cell was associated with MF progression and dysfunction.<sup>17</sup> Immunotherapy that targets CD4<sup>+</sup>T cell guards against fibrosis and dysfunction in the ischemic heart,<sup>18</sup> suggesting that CD4<sup>+</sup>T cell is an attractive novel therapeutic target for MF. The presentation of MHC-II antigens to CD4<sup>+</sup>T cell is a key condition for CD4<sup>+</sup>T cell activation.<sup>19</sup> Due to the expression of MHC-II, dendritic cells (DCs) possess potential capacity to take up exogenous antigens that drives the development of CD4<sup>+</sup>T cell.<sup>20</sup> However, numerous studies have demonstrated that EC participates in CD4<sup>+</sup>T cell activation via MHC-II antigen presentation.<sup>21</sup> It has been confirmed that blocking the presentation of MHC-II antigens to CD4<sup>+</sup>T cell by EC is a potential therapeutic strategy for fibrosis.<sup>14</sup> Consequently, suppression of MHC-II expression in ECs may alleviate MF and could potentially lead to new therapies.

Zhilong Huoxue Tongyu (ZL) capsule (Patent No. 200810147774.1) is a patented Chinese herbal formulation consisting of Astragalus membranaceus, Leech, Earthworm, Cinnamonum cassia, and Sargentodoxa cuneate, having functions of replenishing qi and activating blood, dispelling wind and reducing phlegm.<sup>22</sup> ZL capsule has been used in clinic for more than 20 years as a herbal remedy with definite therapeutic efficacy for the treatment of CVDs.<sup>23</sup> Both clinical trials and animal studies have indicated that ZL capsule can improve coronary blood flow, stabilize plaque, reduce blood lipid, protect the function of myocardial cells and vascular endothelial cells.<sup>24,25</sup> However, the mechanism of its anti-MF is not fully understood.

According to traditional Chinese medicine theory, the main lesion of EC dysfunction is Qi deficiency and blood stasis,<sup>26</sup> corresponding to the function of ZL capsule. In our previous studies, ZL capsule has been proven to exert anti-inflammatory and anti-apoptotic activities to treat CVDs.<sup>22,24</sup> However, inflammatory response is only a pathological manifestation in the early stage of MF, and it is suppressed to some extent after severe heart failure.<sup>27,28</sup> Therefore, the systematic evaluation of the effect of ZL capsule on EC dysfunction during MF is of great significance to understand the pharmacological mechanisms of ZL capsule. In this study, we investigated the beneficial effects of ZL capsule against EC dysfunction *in vivo*, mainly concerning the effect of ZL capsule on the inhibition of endothelial cell-mediated fibroblast activation and inflammatory response, which may shed new lights on its potential

**Table 1**  
Prescription of ZLHXTY capsule.

Scientific Name	Family	English Name	Chinese Name	Part	Used Quantity (Dry Weight)
<i>Whitmania pigra</i> Whitman	Hirudideae	Leech	ShuiZhi	Dried whole body	0.32 g
<i>Pheretima aspergillum</i> (E.Perrier)	Megascolecidae	Earthworm	Dilong	Dried whole body	1.7 g
<i>Astragalus membranaceus</i> (Fisch.) Bge.var.mongholicus (Bge.) Hsiao	Fabaceae	Astragalus	Huang Qi	Roots	2.3 g
<i>Cinnamomum cassia</i> Presl	Lauraceae	Cassia	Gui Zhi	Stem/Twig	0.86 g
<i>Sargentodoxa cuneata</i> (Oliv.) Rehd. Et Wils.	Lardizabalaceae	Sargentglory-vine	DaXueTeng	Stem/Twig	1.7 g

use as a drug candidate for the treatment of MF.

## 2. Materials and methods

### 2.1. Chemicals and reagents

ZL capsules were purchased from the Affiliated Traditional Chinese Medicine Hospital of Southwest Medical University (Luzhou, Sichuan, China, Batch No. 20210619), which consists of a mixture of five TCMs (Table 1). Standard compounds used in quality control analysis including astragaloside A, astragaloside I, astragaloside II, astragaloside III, chlorogenic acid, L-epicatechin, calycosin, wogonin, formononetin, calycosin-7-glucoside, salidroside and ononin were purchased from Beijing Saibaicao Technology Co., Ltd (Beijing, China). Methanol, acetonitrile, formic acid of HPLC-grade were purchased from Thermo Fisher Scientific (Massachusetts, USA). The other chemicals and solvents were of analytical grade. Details of the antibodies used in this study are shown in Table 2.

### 2.2. Sample preparation for UPLC-HR-MS analysis

For the chemical characterization of ZL capsule, the capsule powder was sonicated with 10 times of 70% ethanol for 0.5 h and then 8 times of 70% ethanol for 0.5 h. Finally, the combined supernatants were concentrated by rotary evaporation and freeze vacuum dried to obtain extracts of ZL capsule for subsequent UPLC-HR-MS analysis and animal experiments.<sup>25</sup>

The twelve standard compounds including astragaloside A, astragaloside I, astragaloside II, astragaloside III, chlorogenic acid, L-epicatechin, calycosin, wogonin, formononetin, calycosin-7-glucoside, salidroside and ononin were dissolved in methanol before standard validation of ZL capsule by UPLC-HR-MS.

### 2.3. UPLC-HR-MS conditions for chemical characterization

Chemical characterization of ZL capsule was performed by the ultimate 3000 ultra high performance liquid chromatography (UPLC) system coupled with high resolution Q-Exactive mass

spectrometry (HR-MS) via an electrospray ionization (ESI) interface from Thermo Fisher Scientific (Bremen, Germany). An auto-sampler, a diode-array detector, a column compartment, and two pumps were included in the chromatography system. A BEH C18 column (1.7 m, 2.1 mm ID100 mm, Waters) maintained at 35 °C was selected for separation of ZL capsule extract after the chromatographic parameters were improved. With acetonitrile and water both containing 0.1% formic acid and flowing at a rate of 200 µL/min, the elution gradient was optimized as follows: 0–5 min at 2% B; 8–45 min at 20% B; 45–52 min at 55% B; and 52–55 min at 100% B. The sampler was adjusted to 4 °C, and the injection volume was 2.0 µL.<sup>29,30</sup>

Negative full scan mode was utilized to accurately acquire molecular ions in the range of  $m/z$  70–1050 Da at a resolution of 70,000 in order to identify the components in ZL capsule extract. Spray voltage, –3.0 kV; sheath gas flow rate, 35 arb; aux gas flow rate, 10 arb; capillary temperature, 320 °C; vaporizer temperature, 250 °C; and RF lens, 50% were the other settings. Standards were applied to assist component identification. Xcalibur 4.5 software (Thermo Fisher) was utilized for UPLC-HR-MS control and data handling.<sup>31</sup>

### 2.4. Animals and treatment

The male C57BL/6j mice (20–22 g body weight, 7–8 weeks old) were purchased from GemPharmatech Co. Ltd. They were raised in clean normal cages at a temperature of 22 ± 0.5 °C and a humidity of 55 ± 5%, 12 h alternating light and dark cycle. Mice had free access to a standard diet and drinking water and were cared for humanely. Prior to the trials, animals were adapted to the lab environment for 7 days. The study was approved by the Animal Research Committee of Southwest Medical University (No. 20211115–010).

C57BL/6j mice were intraperitoneally injected with isoproterenol (ISO, 5 mg/kg, MCE. No. 51-30-9) per day for 14 consecutive days, and the control group was given the same amount of normal saline. The prepared ZL capsule extract was dissolved in normal saline according to the dose of 2 ml/100g (crude material content:

**Table 2**  
Description of the antibodies used in this study.

Name	Citation	Supplier	Cat no.	Clone no.
α-Actin	PMID:34099640	Santa Cruz	sc-32251	1A4
Anti-Collagen I	PMID:32814879	abcam	ab34710	Polyclonal
Anti-Collagen III	PMID:35420633	Proteintech	22734-1-AP	Polyclonal
Anti-Mouse CD31	PMID:8980224	BD Biosciences	553370	MEC 13.3
Anti-FSP1	PMID:31634900	Proteintech	20886-1-AP	Polyclonal
Anti-mouse MHC class II	PMID: 35219847	Bioss	Bs-8481R	Polyclonal
Anti-mouse CD4	PMID:35087966	Proteintech	65104-1-Ig	Polyclonal
Anti-IL-1 Beta	PMID:30581532	Proteintech	16806-1-AP	Polyclonal
Anti-mouse IL-6	PMID:20139174	BioLegend	504,512	MP5-20F3
Anti-IL-17	PMID:34974400	Proteintech	66148-1-Ig	Polyclonal
Goat Anti-Mouse IgM (Alexa Fluor® 488)	PMID:33294731	abcam	ab150121	Polyclonal
Goat Anti-Rabbit IgG (Alexa Fluor® 488)	PMID:33474514	abcam	ab150081	Polyclonal
Goat Anti-Mouse IgG (Alexa Fluor® 555)	PMID:32638495	abcam	ab150114	Polyclonal
Donkey Anti-Rabbit IgG (H + L) (Alexa Fluor 555)	PMID 25,036,476	Beyotime	A0453	Polyclonal

1.4 g/kg), and the mice in the treatment group were given drug intervention by gavage, and the mice in the model group were given the same volume of normal saline. The model group were gavaged the same volume of physiological saline. The mice were killed on the 15th day to get the heart tissue of the mice.

### 2.5. Echocardiography

We performed echocardiography experiments to assess cardiac function in mice 4h after the end of the last drug administration of the animals, the mice were anesthetized by isoflurane inhalation and were further placed in a pure oxygen induction chamber containing 1.5–2% isoflurane. Heart rate parameters were recorded by MyLab Sigma VET, the ejection fraction (EF%) and short stroke fraction (FS%) in bidimensional mode were calculated while the left ventricular end-diastolic diameter (LVEDd) and left ventricular end-systolic diameter (LVESd) were measured in M-mode. All experimental protocols have been reported to be expensive in previous studies.<sup>32,33</sup>

### 2.6. Histopathological examinations

The fresh heart tissue was cut into three parts, one part was soaked in 4% paraformaldehyde, one part was embedded in optimal cutting temperature (OCT) gel and frozen in liquid nitrogen while the rest was used for flow cytometry. We fixed the tissue with 4% paraformaldehyde to maintain the inherent cellular morphology and structure of the tissue, and de-embedded the fresh tissue with OCT gel and then flash frozen in liquid nitrogen to maintain the antigen activity of the tissue for later immunofluorescence staining. After soaking in 4% paraformaldehyde for 72 h, we used increasing concentrations of ethanol for tissue dehydration and decreasing concentrations of ethanol for rehydrating paraffin sections before pathological staining. The paraffin sections were stained with Hematoxylin-Eosin (H&E), Masson's trichrome and Sirius red to evaluate the improvement of myocardial fibrosis. HE staining was used to determine the improvement of cardiac tissue structure by ZL capsule, and Sirius Red and Masson staining were used to determine the improvement of collagen deposition in the heart after treatment with ZL capsule.<sup>34</sup>

### 2.7. Immunocytochemistry

The antigen retrieval was performed by microwave after deparaffinization. The endogenous peroxidase was blocked with the endogenous peroxidase blocker (3% H<sub>2</sub>O<sub>2</sub> solution). Bovine serum albumin was used to block the paraffin slices before an overnight antibody incubation. Incubation with enzyme-labeled secondary antibodies was performed to show the specific binding of the first antibody, and positive staining was observed with the DAB substrate kit.<sup>35</sup>

### 2.8. Immunofluorescent staining of cardiac tissue slides

For the immunofluorescence staining assay, frozen myocardial tissue was cut into 4 μm sections and soaked in 4% paraformaldehyde. Slides were firstly fixed with 5% goat serum and treated with the primary antibody for an overnight incubation at 4 °C. Followed by rinsing with PBS, the slides were then incubated with secondary antibody for 1 h. Finally, the sections were counterstained with DAPI, washed with PBS and stored in 20% glycerol before imaging.<sup>36</sup>

### 2.9. Flow cytometry

Collagenase type IX (125 U/mL), collagenase IS (450 U/mL), or hyaluronidase IS (60 U/mL) were used to dissect the mouse heart in a 20 mM HEPES-PBS buffer. Cardiomyocyte suspensions were stained with the designated monoclonal antibodies or an isotype control before being counted using Z2 cytometry beads (Beckman Coulter) (bilegend). LSRFortessa (BD) was used to capture the data and FlowJo software was used to analyze the results (TreeStar).<sup>37</sup>

### 2.10. Statistical analysis

GraphPad Prism 9 was used for data analysis. The mean and standard deviation of all data was displayed. Using a two-tailed *t*-test, statistical analysis of differences between two groups was carried out. *P* values less than 0.05 and 0.01 were considered significant and very significant, respectively, which were noted as \**p* < 0.05 and \*\**p* < 0.01 individually.

## 3. Results

### 3.1. Dysfunction of EC was induced during MF

Prior to experiments, we analyzed a published scRNA-Seq dataset of heart cells<sup>38</sup> and found that the S100a4<sup>+</sup>Pecam1<sup>+</sup>/Aifm2<sup>+</sup>Pecam1<sup>+</sup>(CD31 official name: Pecam1; FSP1 official name: S100a4/Aifm2) endothelial subpopulation was increased during MF (Fig. 1A and B), indicating that EndMT is closely associated with MF. In the same published public data set, we also analyzed the antigen extraction ability of EC and observed an increase in the number of Hla2<sup>+</sup>Pecam1<sup>+</sup> EC subsets, and the activation of CD4<sup>+</sup>T cell was also enhanced (Fig. 1C and D). These data demonstrated that EC dysfunction plays an important role in MF.

### 3.2. Qualitative compound identification of ZL capsule and target prediction of the active compounds

After the chromatographic conditions were optimized, UPLC-HR-MS was used for compound identification in ZL capsule, and the chromatograms were obtained (Fig. 2A). Twelve compounds including astragaloside A, astragaloside I, astragaloside II, astragaloside III, chlorogenic acid, L-epicatechin, calycosin, wogonin, formononetin, calycosin-7-glucoside, salidroside and ononin were confirmed in ZL capsule by standards (Fig. 2B–C). Through the further target analysis of the active components in ZL capsule, we found that eight targets were closely related to EC dysfunction (Fig. 2D), suggesting that ZL capsule has the potential to ameliorate EC dysfunction.

### 3.3. The successful establishment of ISO-induced MF mouse model

To further analyze the effect of ZL capsule on the improvement of EC dysfunction during MF, a mouse model of ISO-induced myocardial injury mimicking MF was used. To establish the model, C57BL/6 mice were injected with ISO (5 mg/kg) for 14 continuous days (Fig. 3A). Due to abnormal MF markers induced by ISO, the extent of fibrosis was evaluated by routine pathological staining and quantitative related fibrosis markers, providing reliable morphological and biochemical data. H&E, Sirius red and Masson staining showed a significant increase in ISO-induced myocardial injury and fibrosis (Fig. 3B). To further assess the degree of fibrosis, the expression of α-SMA and collagen-I/III were assessed by immunohistochemical staining in the heart tissue. These data showed that the expression of collagen I/III was strongly positive, high, and spread widely throughout the fibrotic tissue

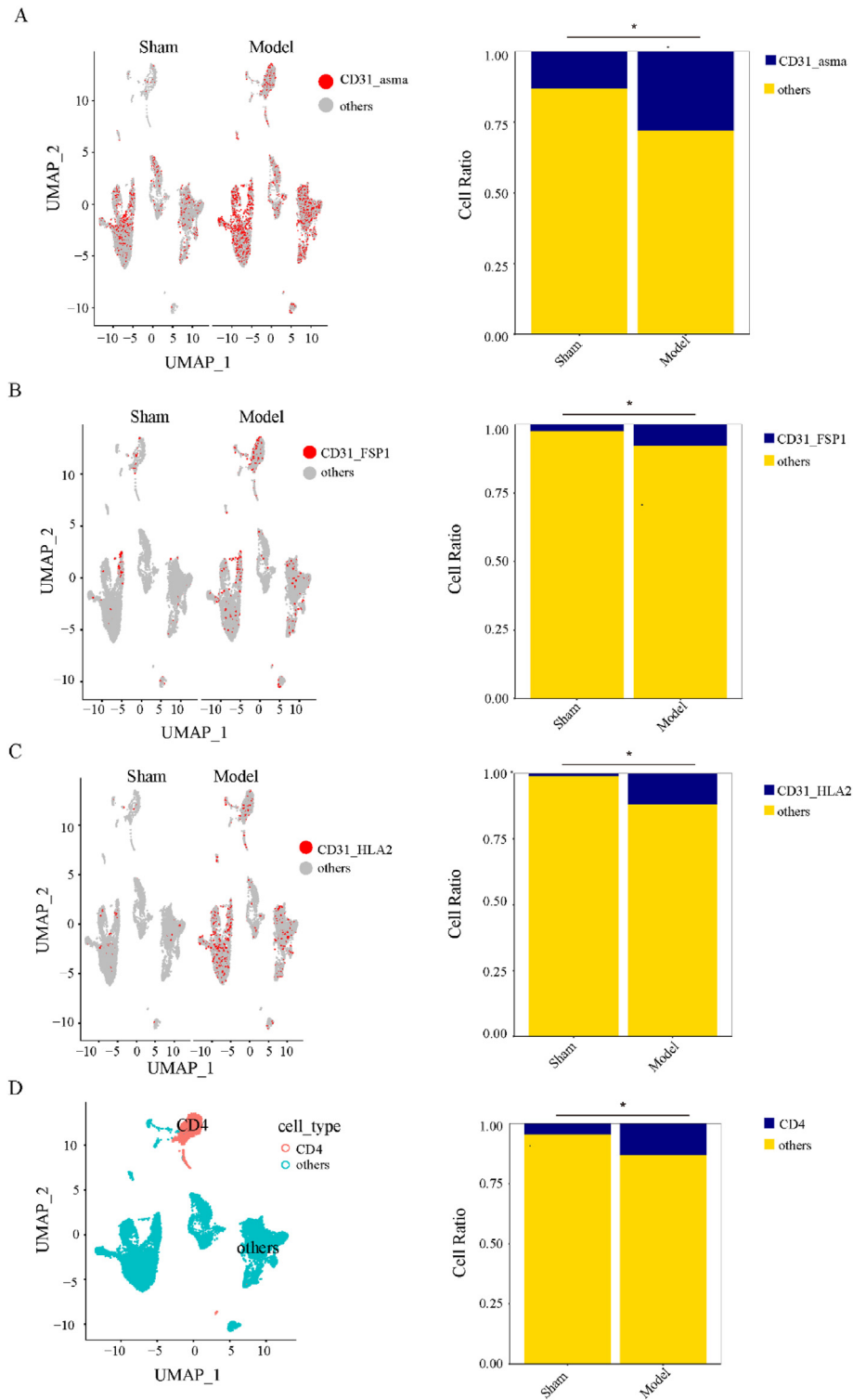
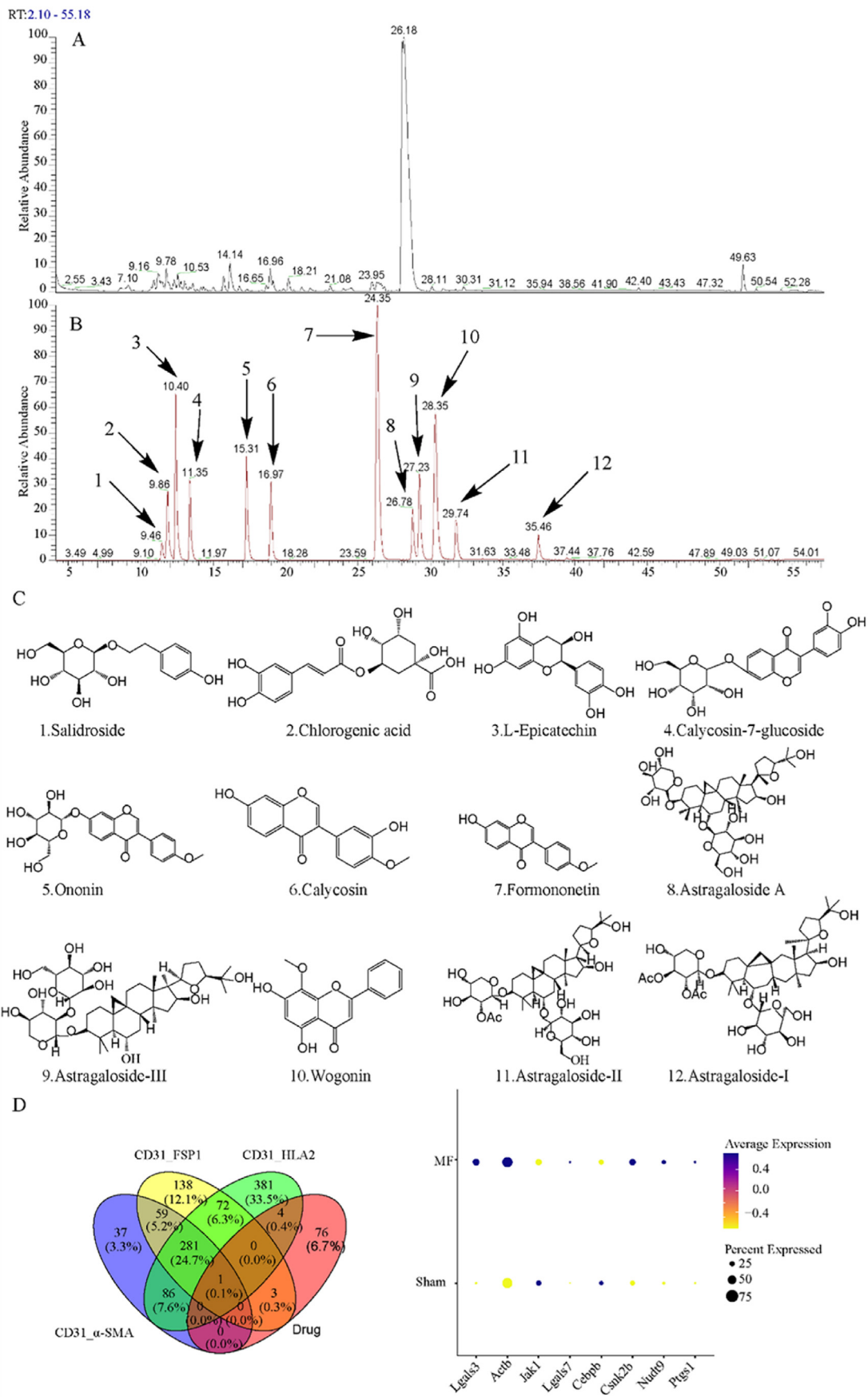


**Fig. 1.** Dysfunction of EC was induced during myocardial fibrosis (A, B) UMAP showing the expression of CD31 and  $\alpha$ -SMA/FSP1 in different pathologies. (C) Quantitative changes of CD31<sup>+</sup>HLA2<sup>+</sup> cell subsets between diseased and normal groups, as determined by single-cell sequencing. (D) Quantification of the frequencies of CD4<sup>+</sup>T cell in two different groups. All of the results are shown as the mean  $\pm$  S.D.; \* $P < 0.05$ ; \*\* $P < 0.01$ .

(Fig. 3C and D), demonstrating the successful establishment of MF model.

#### 3.4. The misexpression of EndMT and endothelial MHC-II antigen presentation to T cells are aggravative during MF

To further determine the role of EC in the process of MF, we performed immunofluorescence staining for evaluating the



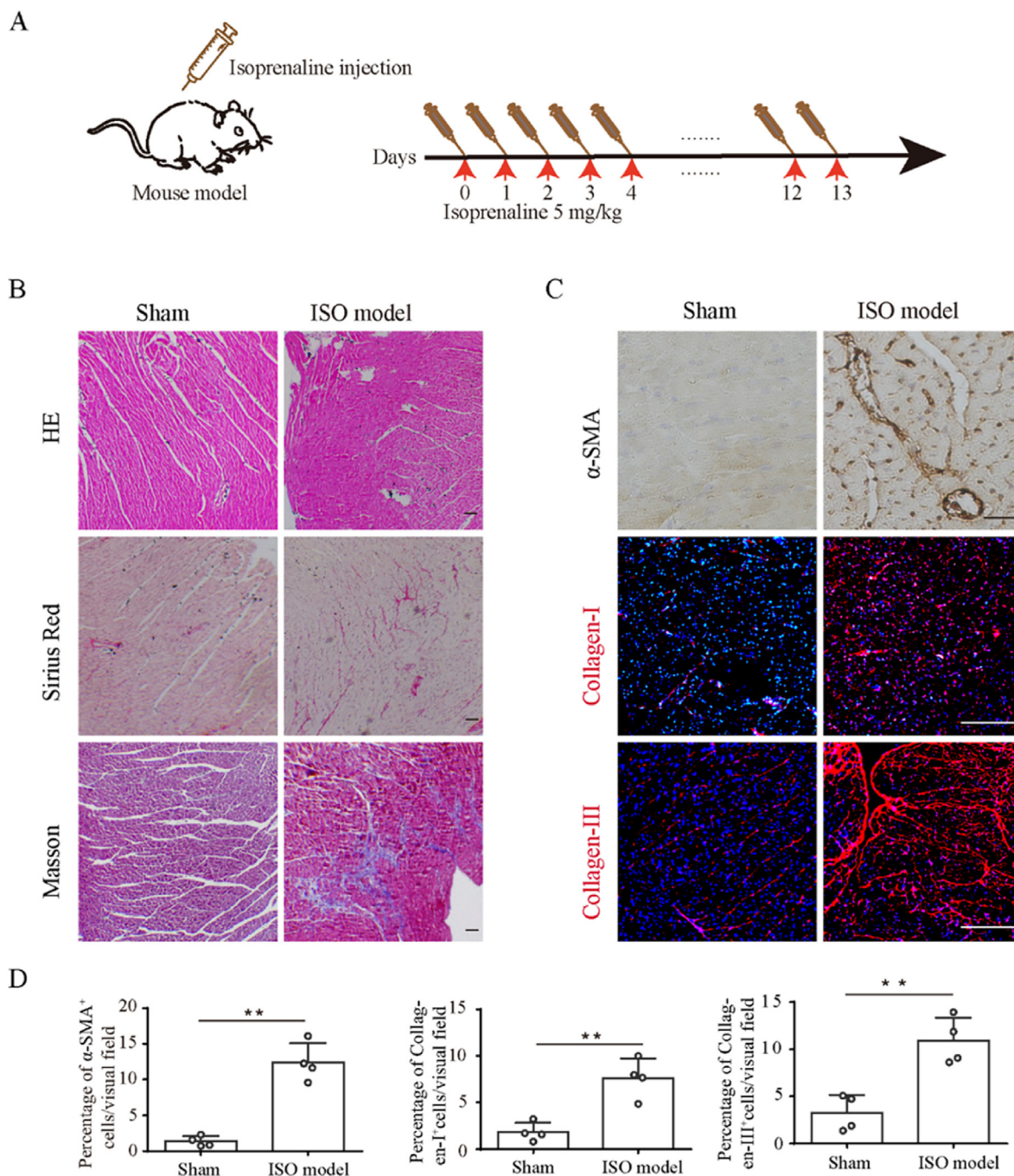


**Fig. 3.** The establishment of ISO-induced MF mouse model was successful.

(A) Process of establishing the present model of mouse myocardium. (B) Histological analysis of myocardial fibrosis. H&E, Sirius Red, and Masson staining results of cardiac tissue (n = 4). Scale bars: 200  $\mu$ m. (C) Immunohistochemical and immunofluorescence analyses of markers ( $\alpha$ -SMA, collagen-I, and collagen-III) related to fibrosis (n = 4). Scale bars: 100  $\mu$ m. (D) Quantification of relative proportion of  $\alpha$ -SMA, collagen-I, and collagen-III cells per visual field for sham and ISO-model (n = 4). All of the results are shown as the mean  $\pm$  S.D.; \*P < 0.05; \*\*P < 0.01.

condition of EndMT and MHC-II. Immunofluorescence analysis of the EC marker CD31 revealed a significant increase in angiogenesis and EndMT in equivalently induced MF (as evidenced by the colocalization of CD31 and the fibroblast marker  $\alpha$ -SMA/FSP1 in

Fig. 4A–C). Consistently, CD31<sup>+</sup> endothelial MHC-II expression was increased in the MF model (Fig. 4D, F). MHC-mediated peptide presentation is essential for adaptive myocardial inflammation because it governs the activation of T cells. Therefore,

**Fig. 2. Qualitative UPLC-HR-MS analysis of ZL capsule**

(A) UPLC-HR-MS chromatogram of ZL capsule in negative ion mode. (B–C) UPLC-HR-MS chromatogram of 12 standards, namely, salidroside (1), chlorogenic acid (2), L-epicatechin (3), calycosin-7-glucoside (4), ononin (5), calycosin (6), formononetin (7), astragaloside A (8), astragaloside III (9), wogonin (10), astragaloside II (11), and astragaloside I (12). (D) Discovery of the eight targets of ZL capsule that are closely related to EC dysfunction.

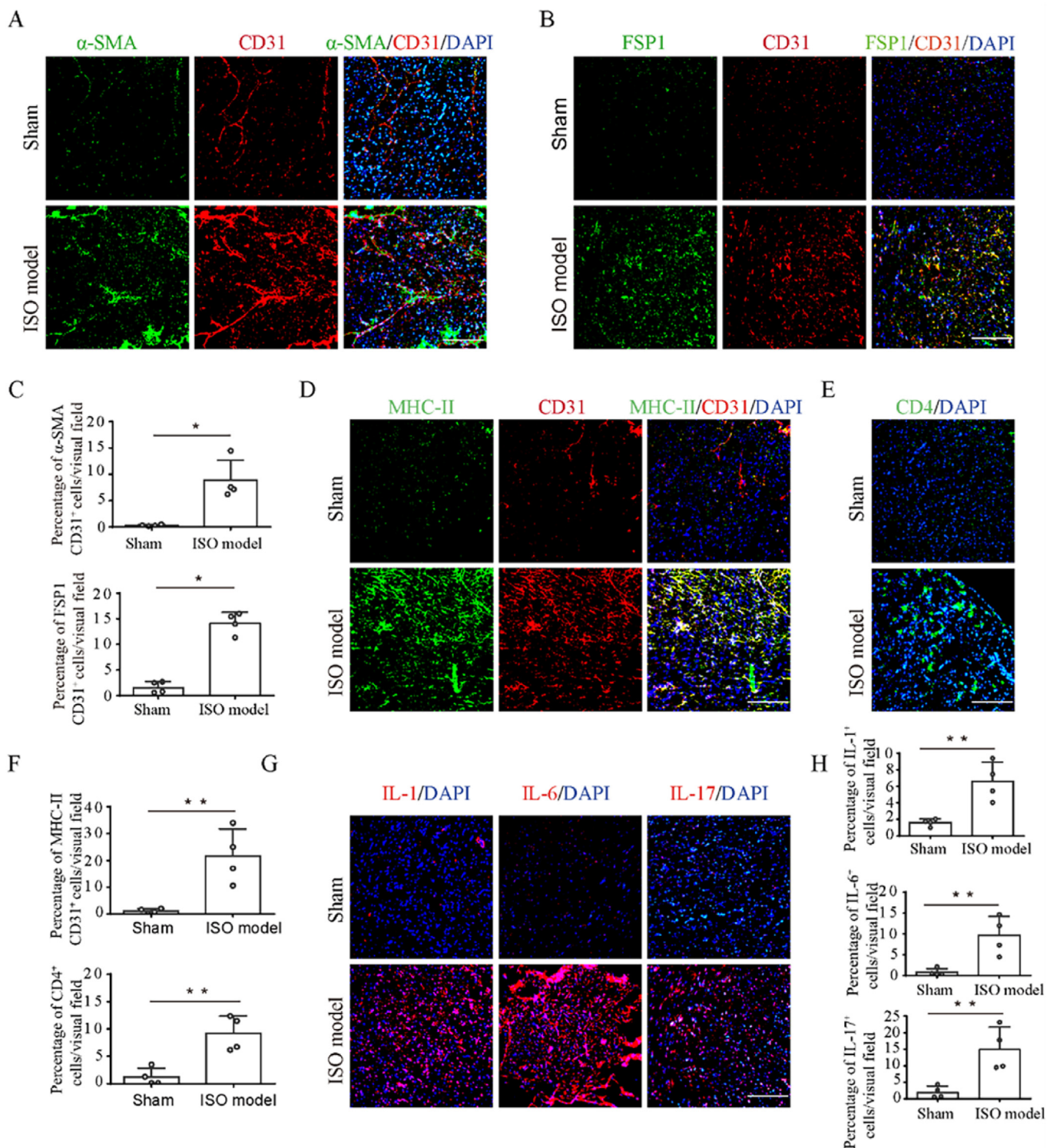


**Fig. 4.** Degree of EndMT and the extent of endothelial MHC-II antigen presentation to T cell are enhanced during myocardial fibrosis. (A) Co-staining of ISO-model or control myocardial sections for the EC marker  $\alpha$ -SMA and the mesenchymal marker FSP1 (n = 4). Scale bars: 100  $\mu$ m. (B) Co-staining of ISO-model or control myocardial sections for CD31 and the mesenchymal marker FSP1 (n = 4). Scale bars: 100  $\mu$ m. (C) Quantification of the numbers of CD31<sup>+</sup> $\alpha$ -SMA<sup>+</sup> and CD31<sup>+</sup>FSP1<sup>+</sup> double-positive cells per visual field. (D) Co-staining of ISO-model or control myocardial sections for CD31 and the MHC class II marker MHC-II (n = 4). Scale bars: 100  $\mu$ m. (E) Immunofluorescent staining against CD4 (green) (n = 4). Scale bars: 100  $\mu$ m. (F) Quantification of the numbers of CD31<sup>+</sup> MHC-II<sup>+</sup> and CD4<sup>+</sup> positive cells per visual field. (G) Immunofluorescent staining against IL-1, IL-6, and IL-17 and counterstaining with DAPI (blue: nuclei) in mouse control and ISO-model myocardial sections (n = 4). Scale bars: 100  $\mu$ m. (H) Quantification of (G) on mouse myocardial sections from the control and ISO-induced myocardial fibrosis mice. All of the results are shown as the mean  $\pm$  S.D.; \**P* < 0.05; \*\**P* < 0.01.



immunofluorescence was used to detect myocardial CD4<sup>+</sup>T cell in each group. The results showed that the number of CD4<sup>+</sup>T cell in MF mice induced by ISO was significantly increased (Fig. 4E). Furthermore, we measured the inflammatory response during the process of MF, and the immunofluorescence staining results showed that the expression of IL-1, IL-6, and IL-17 increased (Fig. 4G–H). Taken together, these results suggest that EC dysfunction is a dangerous risk during MF.

### 3.5. ZL capsule attenuates ISO-induced cardiac dysfunction in mouse models

MyLab Sigma VET is a kind of experimental small animal ultrasound imaging equipment with high frequency and high resolution. Compared with conventional pathological diagnostic techniques for evaluating myocardial fibrosis, MyLab Sigma Vet has the advantage of real-time dynamic monitoring of small animal cardiac function, and has been widely used in the evaluation of the efficacy of anti-myocardial fibrosis drugs. Echocardiography further demonstrated that the MF mice model was successfully established and the cardiac function of the ZL capsule-treated MF mice was improved (Fig. 5A and B). After treatment, left ventricular systolic function was measured by quantitative EF% and FS%. In addition, to further evaluate the degree of fibrosis and the effect of the ZL capsule, LVEDd and LVESd was measured. These results confirmed that ZL capsule can impair cardiac function and improve stress tolerance in ISO-induced heart failure.

### 3.6. ZL capsule attenuates the symptoms of MF

In the ISO-induced MF model, MF was improved in the ZL capsule-treated group. Staining with H&E and Sirius Red showed a significant reduction in MF after administration of ZL capsule. Deposition of  $\alpha$ -SMA and collagen-I/III were also reduced in the group of ZL capsule-treated mice (Fig. 6A and B). As mentioned above, these findings suggest that ZL capsule can inhibit collagen deposition and attenuate the symptoms of MF.

### 3.7. ZL capsule dampens EndMT and endothelial MHC-II antigen presentation to improve MF

To further analyze the effect of ZL capsule on EC dysfunction, the related indexes of pathological vascular remodeling in myocardial tissues were stained. Immunofluorescence staining showed that the co-staining of  $\alpha$ -SMA/FSP1- and CD31-positive area in the myocardium of treated mice were reduced (Fig. 7A–C). At the same time, we also observed that ZL capsule significantly reduced the expression of MHC-II on EC (Fig. 7D–F). These results provided solid evidence that ZL capsule could improve MF by preventing EC dysfunction.

### 3.8. ZL capsule reduces CD4<sup>+</sup>T cell response and inflammation during MF

It was previously reported that MHC-II levels were correlated with the level of CD4<sup>+</sup>T cell responses.<sup>14</sup> In this study, we counted

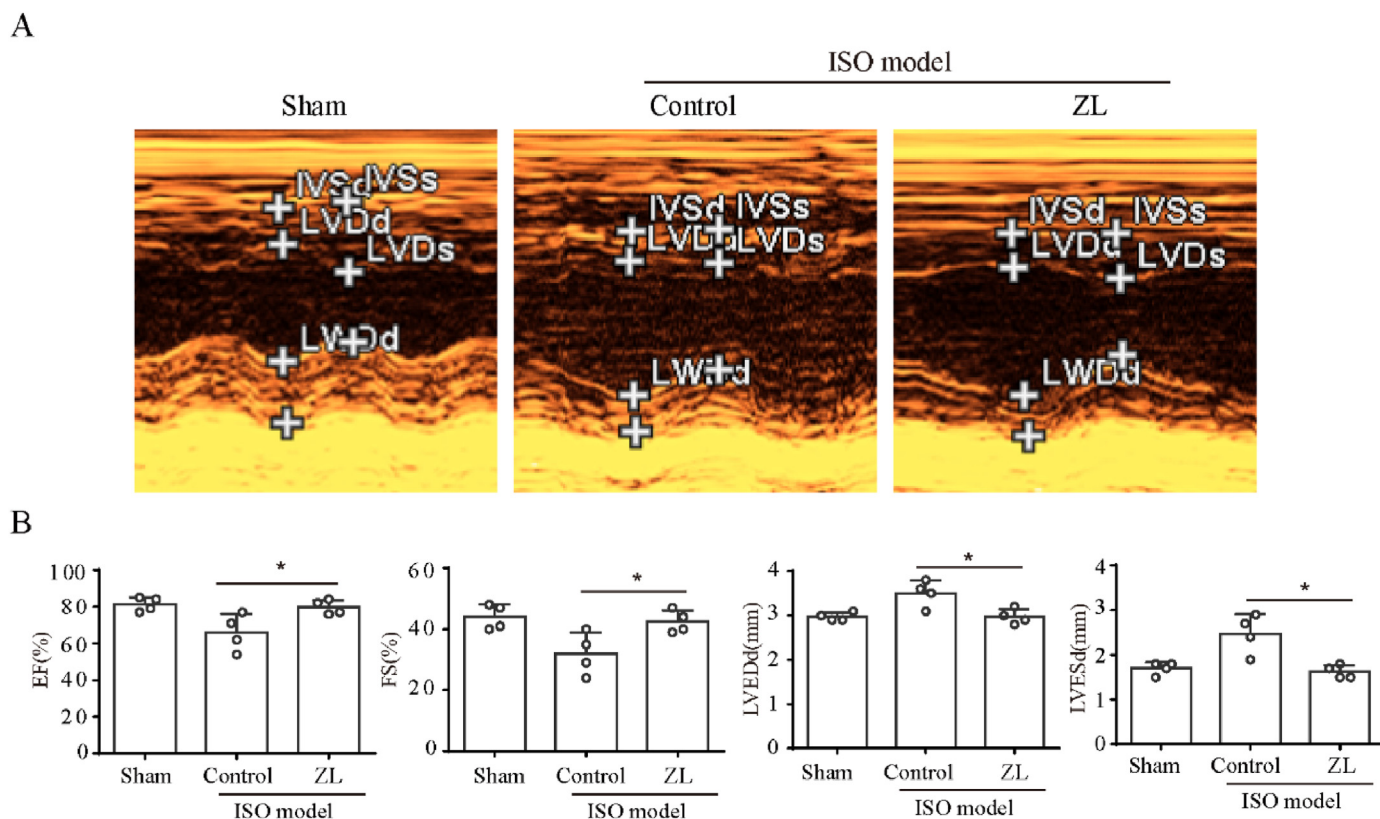


**Fig. 5. ZL capsule improves ISO-induced cardiac dysfunction.** (A) Representative images of echocardiography. (B) Echocardiographic assessment of EF%, FS%, LVESd, and LVEDd by quantification to evaluate the impaired cardiac function (n = 4). All of the results are shown as the mean ± S.D.; \*P < 0.05; \*\*P < 0.01.

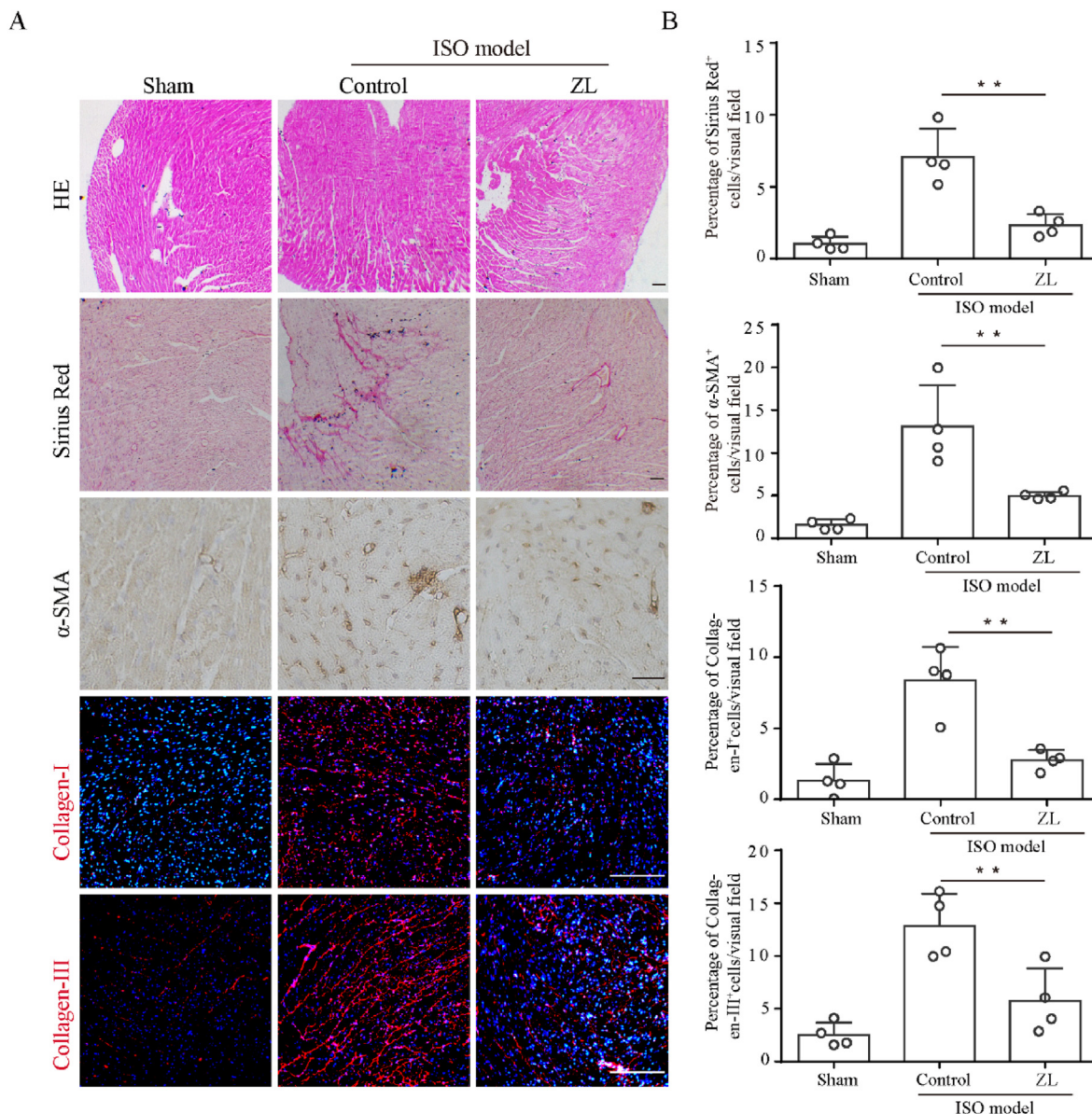


**Fig. 6.** ZL capsule improved myocardial structure and reduced collagen deposition.

(A, B) ZL capsule attenuates a series of symptoms after ISO-induced myocardial fibrosis. H&E, Sirius Red staining (Scale bar: 200  $\mu$ m) and immunohistochemistry against  $\alpha$ -SMA and immunofluorescence of collagen-I/III were performed and quantified in mouse myocardial sections ( $n = 4$ ). Scale bar: 100  $\mu$ m. All of the results are shown as the mean  $\pm$  S.D.; \* $P < 0.05$ ; \*\* $P < 0.01$ .

the number of CD4<sup>+</sup>T cell and observed a significant reduction in CD4<sup>+</sup>T cell counts in the ZL capsule-treated group compared with the control group (Fig. 8A–C), which was consistent with previous reported results.<sup>14</sup> The inflammatory response (IL-1, IL-6, IL-17) mediated by CD4<sup>+</sup>T cell was improved after CD4<sup>+</sup>T cell was inhibited (Fig. 8D and E). Collectively, these data showed that ZL capsule can significantly improve the inflammatory response mediated by EC dysfunction.

#### 4. Discussion

MF is known to play a key role in the pathogenic remodeling of myocardial ischemia, hypertension, and heart failure.<sup>39</sup> EC dysfunction mediated myofibrotic cell activation and inflammatory response are important factors that aggravate the formation of myocardial fibrogenesis during cardiac remodeling.<sup>40</sup> In this study,

we proved that ZL capsule could ameliorate MF by ameliorating EC dysfunction in an ISO-induced mouse model of MF. As far as we know, it was firstly confirmed that ZL capsule has the potential to be an anti-fibrotic drug by improving EC dysfunction (Fig. 9).

A large number of basic and clinical studies have proven that ZL capsule has a positive effect on CVDs.<sup>22,25</sup> Our previous study showed that ZL capsule has protective effects on CVDs in a dose dependent manner.<sup>25</sup> In this study, we used echocardiography to systematically evaluate the improvement of ZL capsule on the cardiac function in mice. The results showed that ZL capsule significantly increased the myocardial EF% and FS% of ISO-induced mice, and obviously reduced LVEDd and LVESd. It was further confirmed that ZL capsule could improve the cardiac function of mice at the animal level. Consequently, treatment with ZL capsule can significantly enhance the cardiac function of mice and reduce the symptoms of MF.

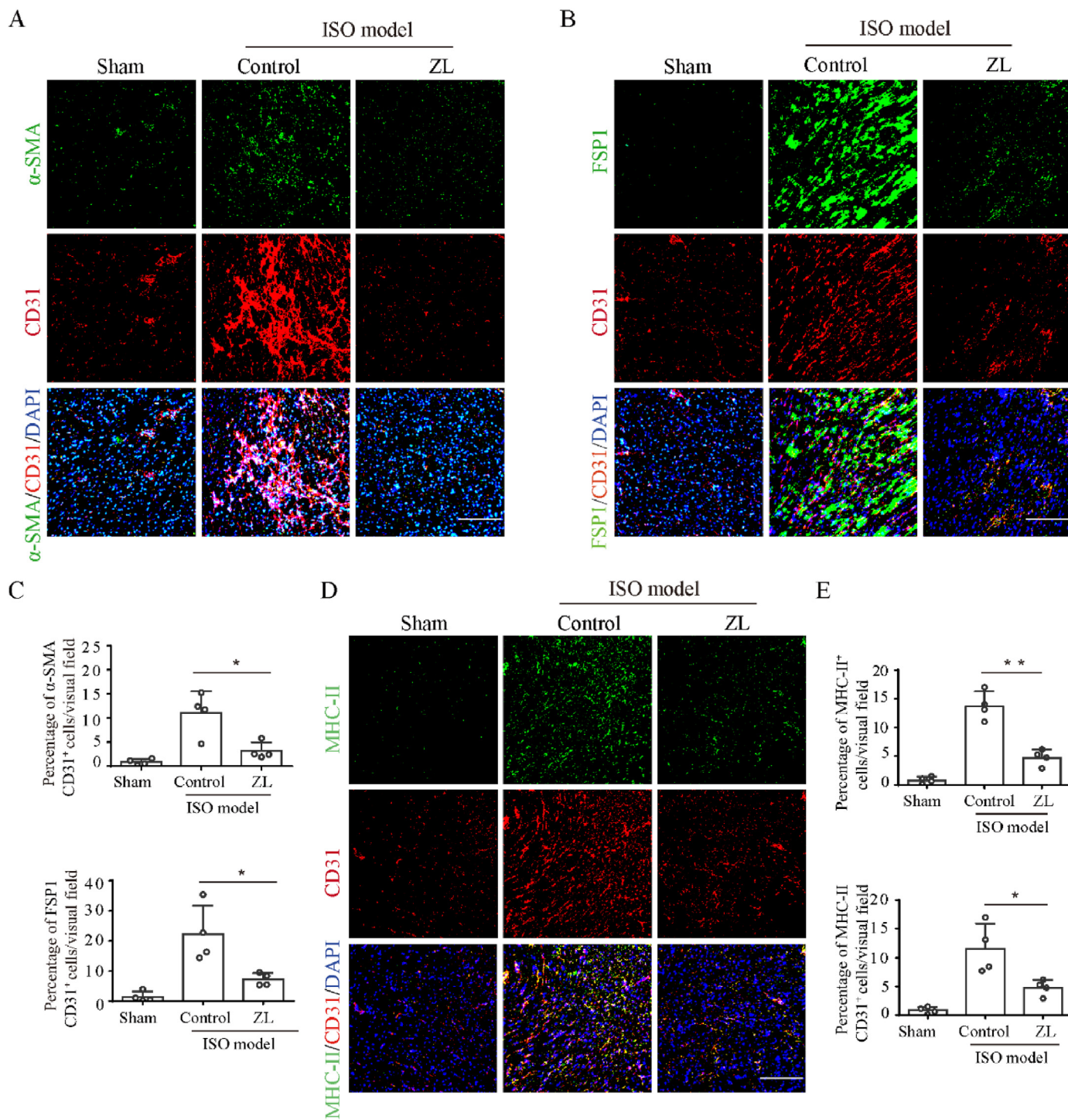


**Fig. 7. ZL capsule can inhibit EndMT and the expression of MHC-II of EC.**

(A–C) Co-staining of sections from the ISO-induced myocardial fibrosis model for the EC marker CD31 and the mesenchymal markers α-SMA and FSP1, and quantification of the numbers of CD31+α-SMA+ and CD31+FSP1+ double-positive cells per visual field. (D–E) Co-staining of CD31 and the MHC class-II markers MHC-II, and quantification of the numbers of CD31+ MHC-II+ double-positive cells per visual field. Scale bar: 100 μm. All of the results are shown as the mean ± S.D.; \*P < 0.05; \*\*P < 0.01.

The key features of fibrosis are increased collagen content, and the arrangement of the collagen fibers becomes disordered. The accumulation of collagen fibers in the heart is one of the main manifestations of MF, the presence of a collagen scar increases stiffness of the myocardial tissue and reduces the ability of the heart to contract.<sup>41</sup> Therefore, reducing the excessive deposition of collagen is an important goal for the treatment of MF. In this study,

in order to systematically evaluate the effect of ZL capsule on MF, routine pathological staining and immunohistochemical staining were performed on mouse myocardial tissues. H&E staining results showed that after ZL capsule treatment, the original disordered heart tissue structure of the MF mice became orderly. Sirius red, Masson's trichrome, and immunohistochemical staining showed that ZL capsule reduced collagen production during fibrosis

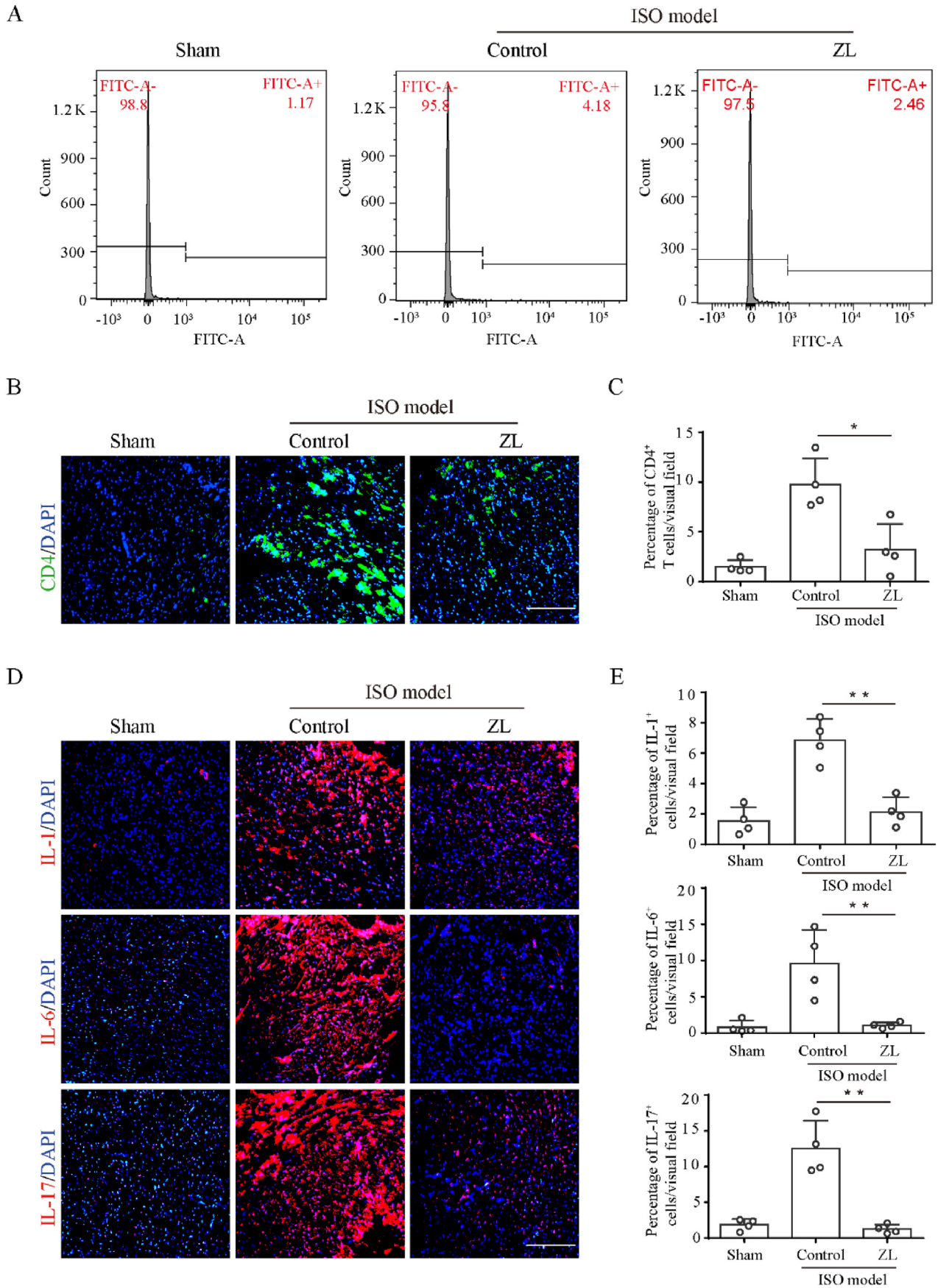


**Fig. 8.** ZL capsule inhibited the action of CD4<sup>+</sup>T cell and inflammatory reaction during myocardial fibrosis. (A) Flow cytometric analysis of the percentage of CD4<sup>+</sup>T cell in cardiac muscle tissues from the indicated experimental groups. (B, C) Immunofluorescent staining and quantification of CD4<sup>+</sup> (red) T cell in mice after treatment with ZL capsule (n = 4). Scale bar: 100  $\mu$ m. (D, E) Immunofluorescent staining and quantification of the number of IL-1<sup>+</sup>, IL-6<sup>+</sup>, and IL-17<sup>+</sup> positive cells per visual field in mouse myocardium (n = 4). All of the results are shown as the mean  $\pm$  S.D.; \* $P$  < 0.05; \*\* $P$  < 0.01.

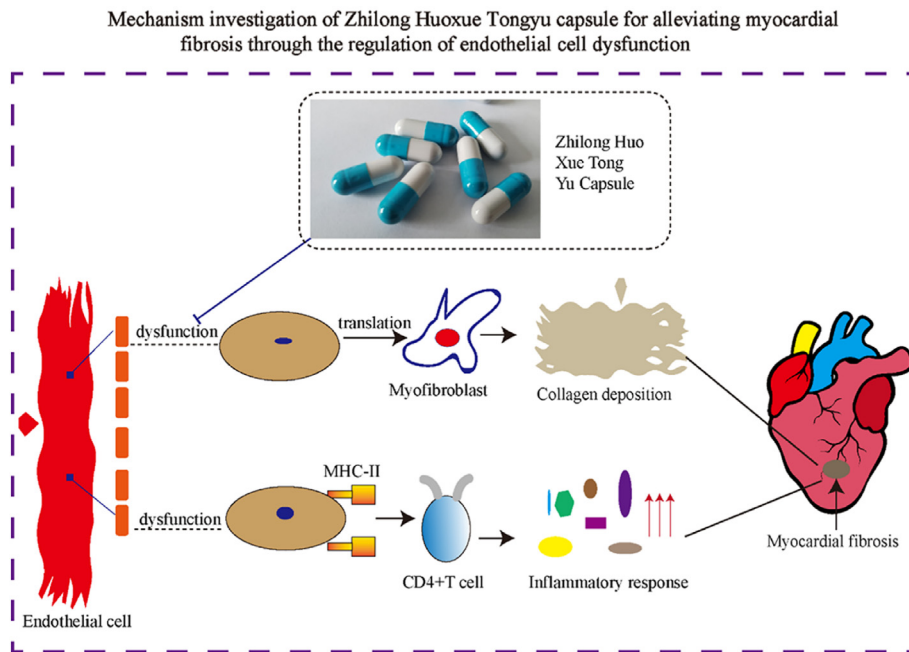


**Fig. 9.** Schematic showing the complex mechanism of ZL capsule for reducing MF. Note 1. ZL capsule can inhibit the activation of myofibroblast cells by inhibiting EndMT, thereby reducing collagen deposition to improve myocardial fibrosis. Note 2. ZL capsule can attenuate the inflammatory response during fibrosis by intervening the activation of CD4<sup>+</sup>T cells mediated by EC.

**Table 3**  
The final results of this study.

Zhilong Huoxue Tongyu capsule alleviates myocardial fibrosis by improving endothelial cell dysfunction	
<b>Section1:</b> Dysfunction of EC was induced during MF	<b>Section2:</b> Qualitative compound identification of ZL capsule and target prediction of the active compounds
<b>Section3:</b> The successful establishment of ISO-induced MF mouse model	<b>Section4:</b> The misexpression of EndMT and endothelial MHC-II antigen presentation to T cells are aggravative during MF
<b>Section5:</b> ZL capsule attenuates ISO-induced cardiac dysfunction in mouse models	<b>Section6:</b> ZL capsule attenuates the symptoms of MF
<b>Section7:</b> ZL capsule dampens EndMT and endothelial MHC-II antigen presentation to improve MF	<b>Section8:</b> ZL capsule reduces CD4 <sup>+</sup> T cell response and inflammation during MF

formation. The above experimental results indicated that ZL capsule had a positive effect on inhibiting the excessive deposition of collagen and improving the myocardial tissue structure during cardiac remodeling.

Previous research has demonstrated that EC has a variety of impacts on the production of fibrosis and the healing of myocardial tissue during cardiac remodeling.<sup>42</sup> The primary process causing angiogenesis, which is crucial for myocardial healing during myocardial infarction, is the clonal growth of resident cardiac EC.<sup>43</sup> Under constant pressure, EC will transform and lose their normal function, turning into a group of dangerous cell subsets that stimulate inflammation to continuously increase collagen-I deposition and promote the development of fibrosis symptoms.<sup>44</sup> The niche formed by EC plays a guiding role in collagen deposition during fibrosis.<sup>45</sup> In our research, we focus on the alleviation effects of ZL capsule on EC dysfunction during MF. According to the results, ZL capsule interferes with EC dysfunction in many ways, among which, it has a better inhibitory effect on EndMT. The number of myofibrotic cells and collagen production were observed to be dramatically reduced during the fibrosis process in mice treated with ZL capsule, indicating that ZL capsule could directly reduce collagen synthesis by mediating the transformation of EC into myofibrotic cells. We also evaluated the influence of ZL capsule on

other functions of EC, and the results showed that ZL capsule also had a beneficial effect on improving EC-mediated inflammatory response via inhibiting the expression of EC MHC complex, preventing CD4<sup>+</sup>T cell activation and reducing the inflammatory response during fibrosis (Table 3).

EC dysfunction can promote fibrosis in many aspects. In addition to EndMT and EC mediated inflammation, exosomes secreted by EC and vascular thinning and vascular senescence induced by EC are also important factors for participating in the formation of fibrosis.<sup>46,47</sup> Therefore, ameliorating EC dysfunction to alleviate MF symptoms may be an ideal treatment for CVDs. In the future, whether ZL capsule can improve other aspects of EC dysfunction remains to be further investigated.

### 5. Conclusion

The ZL capsule is a well-known traditional Chinese herbal remedy for CVDs. The present study clarified the mechanisms of ZL capsule for improving CVDs using *in vivo* ISO-induced MF model. We further demonstrated that ZL capsule can inhibit EndMT and block the inflammatory response mediated by endothelial antigen presentation to improve fibrosis. Taken together, these findings provide a new clue to exploit the TCM formula ZL capsule for its

potential therapeutic utilization in MF.

### Data availability

The data used to support the findings of this study are included within the article. The supporting data is available upon reasonable request from the corresponding author.

### Authors' contributions

**Tao Bi:** Writing original draft, Methodology, Investigation, Supervision. **Yanan Zhou:** Investigation, Preparation, Methodology, Data curation. **Linshen Mao:** Methodology, Investigation. **Pan Liang:** Methodology, Investigation. **Jiali Liu:** Methodology, Investigation. **Luyin Yang:** Methodology, Investigation. **Guilin Ren:** Methodology, Investigation. **Maryam Mazhar:** Writing—review & editing. **Hongping Shen:** Funding acquisition. **Ping Liu:** Funding acquisition. **Roman Spáčil:** Writing—review & editing. **Qing Guo:** Methodology, Investigation. **Gang Luo:** Conceptualization, Supervision, Writing—review & editing. **Sijin Yang:** Conceptualization, Funding acquisition, Supervision. **Wei Ren:** Conceptualization, Funding acquisition, Supervision, Writing—review & editing.

### Ethics statement

This study was carried out in accordance with the recommendations of regulations of the experimental animal ethics committee of Southwest Medical University. The protocol was approved by the experimental animal ethics committee of Southwest Medical University (No.20211115–010).

### Funding acknowledgments

This research was funded by Sichuan Administration of Traditional Chinese Medicine (Number: 2023MS379), Sichuan Science and Technology Program (Number: 2022YFS0635, 2022YFS0618), Innovation Team and Talents Cultivation Program of National Administration of Traditional Chinese Medicine (Number: ZYYCXTD-C-202207), Innovation Team of Sichuan Administration of Traditional Chinese Medicine (Number: 2022C007).

### Declaration of competing interest

The authors declare that there are no financial conflicts of interest in regard to this work.

### Acknowledgments

Thanks for the experiment conditions provided by Luzhou Key Laboratory for Prevention and Treatment of Cardiovascular and Cerebrovascular Diseases with Integrated Traditional Chinese and Western Medicine and the High-resolution Mass Spectrometry Testing Center of the Affiliated Traditional Chinese Medicine Hospital of Southwest Medical University.

### References

1. Yan F, Sun Y, Mao Y, et al. Ultrasound molecular imaging of atherosclerosis for early diagnosis and therapeutic evaluation through leucocyte-like multiple targeted microbubbles. *Theranostics*. 2018;8(7):1879–1891.
2. Roth GA, Mensah GA, Johnson CO, et al. Global burden of cardiovascular diseases and risk factors, 1990–2019: update from the GBD 2019 study. *J Am Coll Cardiol*. 2020;76(25):2982–3021.

3. Aimo A, Gaggin HK, Barison A, Emdin M, Januzzi Jr JL. Imaging, biomarker, and clinical predictors of cardiac remodeling in heart failure with reduced ejection fraction. *JACC Heart Fail*. 2019;7(9):782–794.
4. Zhu ZD, Ye JM, Fu XM, et al. DDAH2 alleviates myocardial fibrosis in diabetic cardiomyopathy through activation of the DDAH/ADMA/NOS/NO pathway in rats. *Int J Mol Med*. 2019;43(2):749–760.
5. Zong Y, Huang Y, Chen S, et al. Downregulation of endogenous hydrogen sulfide pathway is involved in mitochondrion-related endothelial cell apoptosis induced by high salt. *Oxid Med Cell Longev*. 2015;2015:754670.
6. Siasos G, Sara JD, Zaromytidou M, et al. Local low shear stress and endothelial dysfunction in patients with nonobstructive coronary atherosclerosis. *J Am Coll Cardiol*. 2018;71(19):2092–2102.
7. Eirin A, Ebrahimi B, Kwon SH, et al. Restoration of mitochondrial cardiolipin attenuates cardiac damage in swine renovascular hypertension. *J Am Heart Assoc*. 2016;5(6).
8. Morganti M, Carpi A, Nicolini A, et al. Atherosclerosis and cancer: common pathways on the vascular endothelium. *Biomed Pharmacother*. 2002;56(7):317–324.
9. Nagai N, Ohguchi H, Nakaki R, et al. Downregulation of ERG and FLI1 expression in endothelial cells triggers endothelial-to-mesenchymal transition. *PLoS Genet*. 2018;14(11):e1007826.
10. Wang J, Yu M, Xu J, et al. Glucagon-like peptide-1 (GLP-1) mediates the protective effects of dipeptidyl peptidase IV inhibition on pulmonary hypertension. *J Biomed Sci*. 2019;26(1):6.
11. Lovisa S, Fletcher-Sanankone E, Sugimoto H, et al. Endothelial-to-mesenchymal transition compromises vascular integrity to induce Myc-mediated metabolic reprogramming in kidney fibrosis. *Sci Signal*. 2020;13(635).
12. Wang B, Ge Z, Wu Y, et al. MFG8 is down-regulated in cardiac fibrosis and attenuates endothelial-mesenchymal transition through Smad2/3-Snail signalling pathway. *J Cell Mol Med*. 2020;24(21):12799–12812.
13. Carambia A, Frenzel C, Bruns OT, et al. Inhibition of inflammatory CD4 T cell activity by murine liver sinusoidal endothelial cells. *J Hepatol*. 2013;58(1):112–118.
14. Zhang Y, Yang X, Bi T, et al. Targeted inhibition of the immunoproteasome blocks endothelial MHC class II antigen presentation to CD4(+) T cells in chronic liver injury. *Int Immunopharm*. 2022;107:108639.
15. Weirather J, Hofmann UD, Beyersdorf N, et al. Foxp3+ CD4+ T cells improve healing after myocardial infarction by modulating monocyte/macrophage differentiation. *Circ Res*. 2014;115(1):55–67.
16. Lu M, Qin X, Yao J, Yang Y, Zhao M, Sun L. Th17/Treg imbalance modulates rat myocardial fibrosis and heart failure by regulating LOX expression. *Acta Physiol*. 2020;230(3):e13537.
17. Zarak-Crnkovic M, Kania G, Jazwa-Kusior A, et al. Heart non-specific effector CD4(+) T cells protect from postinflammatory fibrosis and cardiac dysfunction in experimental autoimmune myocarditis. *Basic Res Cardiol*. 2019;115(1):6.
18. Savvatis K, Pappritz K, Becher PM, et al. Interleukin-23 deficiency leads to impaired wound healing and adverse prognosis after myocardial infarction. *Circ Heart Fail*. 2014;7(1):161–171.
19. Kinzel S, Lehmann-Horn K, Torke S, et al. Myelin-reactive antibodies initiate T cell-mediated CNS autoimmune disease by opsonization of endogenous antigen. *Acta Neuropathol*. 2016;132(1):43–58.
20. Li H, Hong S, Qian J, Zheng Y, Yang J, Yi Q. Cross talk between the bone and immune systems: osteoclasts function as antigen-presenting cells and activate CD4+ and CD8+ T cells. *Blood*. 2010;116(2):210–217.
21. Gkoutidi AO, Garnier L, Dubrot J, et al. MHC class II antigen presentation by lymphatic endothelial cells in tumors promotes intratumoral regulatory T cell-suppressive functions. *Cancer Immunol Res*. 2021;9(7):748–764.
22. Liang P, Mao L, Ma Y, Ren W, Yang S. A systematic review on Zhilong Huoxue Tongyu capsule in treating cardiovascular and cerebrovascular diseases: pharmacological actions, molecular mechanisms and clinical outcomes. *J Ethnopharmacol*. 2021;277:114234.
23. Li N, Sun J, Chen JL, Bai X, Wang TH. Gene network mechanism of Zhilong Huoxue Tongyu capsule in treating cerebral ischemia-reperfusion. *Front Pharmacol*. 2022;13:912392.
24. Liu M, Pu Y, Gu J, et al. Evaluation of Zhilong Huoxue Tongyu capsule in the treatment of acute cerebral infarction: a systematic review and meta-analysis of randomized controlled trials. *Phytomedicine*. 2021;86:153566.
25. Mazhar M, Yang G, Mao L, et al. Zhilong Huoxue Tongyu capsules ameliorate early brain inflammatory injury induced by intracerebral hemorrhage via inhibition of canonical NF- $\kappa$ B signaling pathway. *Front Pharmacol*. 2022;13:850060.
26. Chen B, Tie MH, Wei DX, Chen WJ, Gong RY. To explore the etiology and pathogenesis of vascular endothelial dysfunction of hypertension based on the theory of "Yin and Yang imbalance". *Chin J Integr Med Cardio Cerebrovasc Dis*. 2021;19(13):2281–2284.
27. Bacmeister L, Schwarzl M, Warnke S, et al. Inflammation and fibrosis in murine models of heart failure. *Basic Res Cardiol*. 2019;114(3):19.
28. Prabhu SD, Frangogiannis NG. The biological basis for cardiac repair after myocardial infarction: from inflammation to fibrosis. *Circ Res*. 2016;119(1):91–112.

29. Ren W, Chen S, Li S, et al. Photoluminescence enhancement of carbon dots by surfactants at room temperature. *Chemistry*. 2018;24(59):15806–15811.
30. Ren W, Han L, Luo M, et al. Multi-component identification and target cell-based screening of potential bioactive compounds in toad venom by UPLC coupled with high-resolution LTQ-Orbitrap MS and high-sensitivity Qtrap MS. *Anal Bioanal Chem*. 2018;410(18):4419–4435.
31. Liang P, Ma Y, Yang L, et al. Uncovering the mechanisms of active components from toad venom against hepatocellular carcinoma using untargeted metabolomics. *Molecules*. 2022;27(22).
32. Sun TL, Li WQ, Tong XL, Liu XY, Zhou WH. Xanthohumol attenuates isoprenaline-induced cardiac hypertrophy and fibrosis through regulating PTEN/AKT/mTOR pathway. *Eur J Pharmacol*. 2021;891:173690.
33. Zhao Y, Jiang Y, Chen Y, et al. Dissection of mechanisms of Chinese medicinal formula Si-Miao-Yong-an decoction protects against cardiac hypertrophy and fibrosis in isoprenaline-induced heart failure. *J Ethnopharmacol*. 2020;248:112050.
34. Qing J, Ren Y, Zhang Y, et al. Dopamine receptor D2 antagonism normalizes profibrotic macrophage-endothelial crosstalk in non-alcoholic steatohepatitis. *J Hepatol*. 2022;76(2):394–406.
35. Chaiwong S, Chatturong U, Chanasong R, et al. Dried mulberry fruit ameliorates cardiovascular and liver histopathological changes in high-fat diet-induced hyperlipidemic mice. *J Tradit Complement Med*. 2021;11(4):356–368.
36. Zeng H, Pan T, Zhan M, et al. Suppression of PFKFB3-driven glycolysis restrains endothelial-to-mesenchymal transition and fibrotic response. *Signal Transduct Targeted Ther*. 2022;7(1):303.
37. Lee S, Lee DH, Park BW, et al. In vivo transduction of ETV2 improves cardiac function and induces vascular regeneration following myocardial infarction. *Exp Mol Med*. 2019;51(2):1–14.
38. Wang ZN, Cui M, Shah AM, et al. Cell-type-specific gene regulatory networks underlying murine neonatal heart regeneration at single-cell resolution. *Cell Rep*. 2020;33(10):108472.
39. Chen X, Tang YJ, Gao M, Qin SG, Zhou JZ, Li XH. Prenatal exposure to lipopolysaccharide results in myocardial fibrosis in rat offspring. *Int J Mol Sci*. 2015;16(5):10986–10996.
40. Li Q, Ouyang XY, Lin J. The impact of periodontitis on vascular endothelial dysfunction. *Front Cell Infect Microbiol*. 2022;12:998313.
41. Meng GL, Zhu JB, Xiao YJ, et al. Hydrogen sulfide donor GYY4137 protects against myocardial fibrosis. *Oxid Med Cell Longev*. 2015;2015:691070.
42. Wilhelmi T, Xu XB, Tan XY, et al. Serelaxin alleviates cardiac fibrosis through inhibiting endothelial-to-mesenchymal transition via RXFP1. *Theranostics*. 2020;10(9):3905–3924.
43. Lang CI, Döring P, Gäbel R, et al. [(68)Ga]-NODAGA-RGD positron emission tomography (PET) for assessment of post myocardial infarction angiogenesis as a predictor for left ventricular remodeling in mice after cardiac stem cell therapy. *Cells*. 2020;9(6):1358.
44. Testai L, Brancaleone V, Flori L, Montanaro R, Calderone V. Modulation of EndMT by hydrogen sulfide in the prevention of cardiovascular fibrosis. *Antioxidants*. 2021;10(6):910.
45. Chen Y, Pu Q, Ma Y, et al. Aging reprograms the hematopoietic-vascular niche to impede regeneration and promote fibrosis. *Cell Metabol*. 2021;33(2):395–410 e394.
46. van Balkom BWM, Eisele AS, Pegtel DM, Bervoets S, Verhaar MC. Quantitative and qualitative analysis of small RNAs in human endothelial cells and exosomes provides insights into localized RNA processing, degradation and sorting. *J Extracell Vesicles*. 2015;4:26760.
47. Childs BG, Durik M, Baker DJ, van Deursen JM. Cellular senescence in aging and age-related disease: from mechanisms to therapy. *Nat Med*. 2015;21(12):1424–1435.